JOURNAL OF AIRCRAFT
Vol. 46, No. 4, July–August 2009

Engineering Notes

ENGINEERING NOTES are short manuscripts describing new developments or important results of a preliminary nature. These Notes should not exceed 2500 words (where a figure or table counts as 200 words). Following informal review by the Editors, they may be published within a few months of the date of receipt. Style requirements are the same as for regular contributions (see inside back cover).

Surface Streamlines and Normal-to-Plane Motion Adjacent to a Delta-Wing Planform

M. Elkhoury* and Z. Nakad†
Lebanese American University, Byblos, Lebanon

DOI: 10.2514/1.42154

I. Introduction

THERE has been a growing interest in the investigation and control of flow structure over unmanned combat air vehicles with delta-wing configurations having low-to-moderate sweep angles. Gordnier and Visbal [1] numerically investigated the averaged and instantaneous flow patterns as well as surface flow topology on a moderately swept delta ($\Lambda = 50$ deg) wing. The near-surface topology and buffeting phenomena for the same configuration were experimentally investigated by Taylor and Gursul [2]. A stereoscopic particle image velocimetry (PIV) technique was employed by Ol and Gharib [3] at several crossflow locations to analyze the three-dimensional flow structure of the same delta wing. Investigations of lower sweep angles have been carried out by Yavuz et al. [4] who addressed the near-surface topology and flow structure for a wing of sweep angle $\Lambda = 38.7$ deg. In particular, the effect of wing perturbations and transient motion of flow structure was addressed using a PIV technique applied to near-surface planes. Yavuz and Rockwell [5,6] addressed the effect of trailing-edge jet blowing on cross- and near-surface flow patterns on a delta wing of sweep angle $\Lambda = 35$ deg. The foregoing investigations indicate that control at the trailing edge has a global effect on buffet loading and three-dimensional flow separation. Elkhoury et al. [7] investigated the effect of Reynolds number on the mean and unsteady flow structure of a more complex X-45 planform by employing the PIV technique on crossflow and near-surface planes.

All aforementioned studies addressed near-surface topology by analyzing two-dimensional flow patterns in planes parallel to the planform. To characterize the three-dimensional structure, in particular, the normal-to-plane motion, a stereo PIV version is required. To circumvent this, the near-surface normal-to-plane motion and surface streamlines are determined using a finite difference scheme applied to two-dimensional velocity fields acquired at two planes successively adjacent to a delta-wing planform. To the authors' knowledge, this has not been used in conjunction with the PIV technique to resolve normal-to-plane motion and surface shear stress lines. The technique, which is applicable to all plane solid surfaces, is validated over a representative delta wing using the experimental data of Yavuz and Rockwell [6] collected at two locations (0.5 and 1 mm) above the planform.

Received 12 November 2008; revision received 24 March 2009; accepted for publication 24 March 2009.

*Assistant Professor, Department of Mechanical Engineering, Post Office Box 36; mkhoury@lau.edu.lb.

†Assistant Professor, Department of Electrical and Computer Engineering, Post Office Box 36.

II. Surface Shear Stress Lines And Normal-To-Plane Motion

The present approach is applied to the delta wing of Yavuz and Rockwell [5] which has a sweep angle of $\Lambda = 35$ deg and a chord c of 98 mm. The angle of attack of the planform was $\alpha = 10$ deg with a Reynolds number Re of 10,000 based on the chord. The corresponding freestream velocity U_∞ was 96.8 mm/s. Data acquisition at two laser sheet locations (0.5 and 1 mm) corresponding to $z/c \approx 0.0051$, $z/c \approx 0.0102$, respectively, was necessary for obtaining surface streamlines and normal-to-plane velocity components. Given the 1-mm thickness of the laser sheet, the closest distance away from the planform at which data can be experimentally acquired is 0.5 mm. A schematic of the delta wing showing laser sheet orientation is represented in Fig. 1. All computations were performed using the experimental time-averaged two-dimensional velocity patterns that are based on averaging 200 images of the instantaneous velocity fields collected at each of these locations.

A. Normal-to-Plane Motion near Solid Surfaces

The normal-to-plane motion may be obtained by discretizing the steady, incompressible, differential form of the continuity equation given by

$$\frac{\partial u}{\partial x} + \frac{\partial v}{\partial y} + \frac{\partial w}{\partial z} = 0 \tag{1}$$

Each of the velocity gradients may be discretized at node (i, j, k) using a second-order central difference scheme, for instance,

$$\partial w/\partial z)_{i,j,k} = (w_{i,j,k+1} - w_{i,j,k-1})/2\Delta z + \mathcal{O}(\Delta z^2)$$

Here Δz is the distance separating the two laser sheets and is equal to the distance between the laser sheet and the planform.

The schematic over which Eq. (1) was descretized is shown in Fig. 2a. Note that $\Delta z/c \approx 0.0051$ and the effective resolution, or the normalized grid size, was $\Delta x/c = \Delta y/c \approx 0.0288$. The final discretized form of the continuity equation becomes

$$u_{i+1,j,k} - u_{i-1,j,k} + v_{i,j+1,k} - v_{i,j-1,k} + \frac{\Delta y}{\Delta z}(w_{i,j,k+1} - w_{i,j,k-1}) = 0 \tag{2}$$

The velocity components (u, v) are available from the first laser sheet located above the planform. Furthermore, $w_{i,j,k-1} = 0$ at the wall and the only unknown is the normal-to-plane velocity component at the second laser sheet $w_{i,j,k+1}$, as shown in Fig. 2b. It is clear that Eq. (2) does not resolve the normal-to-plane component at an (i, j, k) node, that is, $w_{i,j,k}$, and therefore it is essential to use the second-order backward difference discretized at node $(i, j, k + 1)$, for instance,

$$\partial w/\partial z)_{i,j,k+1} = (3w_{i,j,k+1} - 4w_{i,j,k} + w_{i,j,k-1})/(2\Delta z) + \mathcal{O}(\Delta z^2)$$

which relates $w_{i,j,k}$ to all known velocities, including $w_{i,j,k+1}$ which was solved in Eq. (2). It is worth noting that using a second-order central difference at the $(k + 1)$ plane results in two unknowns, $w_{i,j,k}$

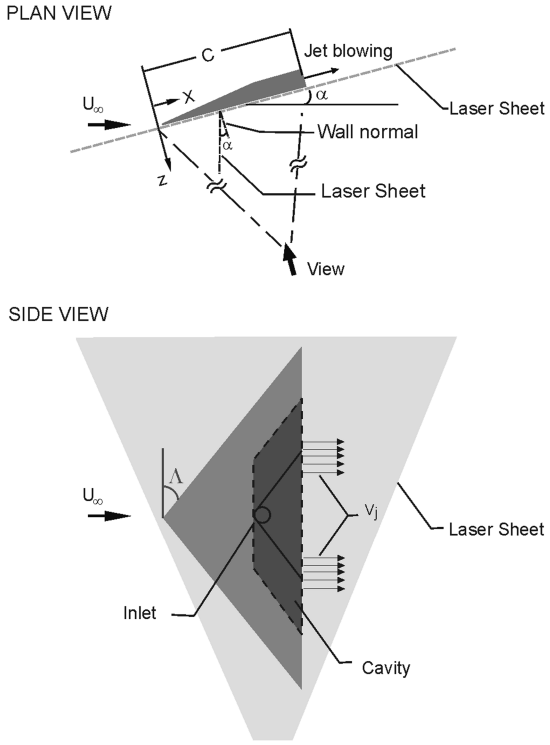

Fig. 1 Delta wing showing jet blowing and laser sheet location.

and $w_{i,j,k+2}$; hence, the backward difference is used. Discretizing the other terms in a similar manner and rearranging to get

$$3u_{i,j,k+1} - 4u_{i-1,j,k+1} + u_{i-2,j,k+1} + 3v_{i,j,k+1} - 4v_{i,j-1,k+1} + v_{i,j-2,k+1} + \frac{\Delta y}{\Delta z}(3w_{i,j,k+1} - 4w_{i,j,k} + w_{i,j,k-1}) = 0 \tag{3}$$

The velocity components (u, v) at the $(k+1)$ plane are made available using the time-averaged values acquired at the second laser sheet location, while $w_{i,j,k+1}$ has already been computed by Eq. (2) and, therefore, Eq. (3) is used to solve for the only unknown, $w_{i,j,k}$.

B. Surface Shear Stress Lines

The surface streamlines can be described by

$$\left(\frac{\mathrm{d}y}{\mathrm{d}x}\right)_{z=0} = \frac{(\partial v/\partial z)_{z=0}}{(\partial u/\partial z)_{z=0}} = \frac{\partial v}{\partial u} \tag{4}$$

where the derivatives are evaluated using a second-order backward difference scheme. In the near vicinity of a planform, an order-of-magnitude analysis of the nondimensional Navier–Stokes equations, performed by the authors, reveals that

$$\frac{\mathrm{d}y}{\mathrm{d}x} = \frac{(\partial p/\partial y)(z/2) + \mu(\partial v/\partial z)_{z=0}}{(\partial p/\partial x)(z/2) + \mu(\partial u/\partial z)_{z=0}} \tag{5}$$

This equation clearly demonstrates the effect of pressure gradient on the streamlines in close vicinity of a planform. It is worth noting the analogy between Eq. (5) and the equation given by Squire [8] for the direction of an oil film streamline

$$\left(\frac{\mathrm{d}y}{\mathrm{d}x}\right)_{\mathrm{oil}} = \frac{(\partial p/\partial y)[(z/2) - h] + \mu(\partial v/\partial z)_{z=h}}{\partial p/\partial x[(z/2) - h] + \mu(\partial u/\partial z)_{z=h}} \tag{6}$$

where h is the oil film thickness above the surface and μ stands for the viscosity of the air. Generally, the pressure gradient term is small compared to the surface shear stress lines and, therefore, oil film patterns are considered as a good representation of the surface shear stress lines [8], an assumption that fails in areas with a high-pressure gradient. It is clear that as the oil's thickness diminishes $h \to 0$, Eq. (6) reduces to Eq. (5). Furthermore, the oil film analysis holds for the present investigation, implying that near-surface streamlines can not be interpreted as surface shear stress lines in the presence of a high-pressure gradient.

III. Normal-to-Plane Motion Adjacent to a Delta-Wing Planform

The normal-to-plane motion is computed using the x-y velocity components obtained from two laser sheets located at $z/c \approx 0.0051$ and $z/c \approx 0.0102$ away from the planform. The calculated values and the values obtained by Yavuz and Rockwell [6] using crossflow imaging located at $x/c = 0.34$ and 0.80, where x is measured from the wing apex, are qualitatively compared. The experimental values were acquired at an angle of attack of 8 deg, whereas the present computation was carried out with an angle of attack of 10 deg. The crossflow imaging was normal to the incoming flow as depicted in Fig. 1, whereas the computed w velocity is normal to the planform, thus a qualitative comparison is more appropriate.

Experimental streamlines, adjacent to the planform at $z/c \approx 0.0051$ are superimposed on the w contours and used to assist in the validation of patterns of w velocity. Contours of dashed and solid lines represent, respectively, negative and positive w, in which the positive sign corresponds to the out-of-plane direction.

The computed w velocity contours for the plane located at $z/c \approx 0.0051$ from the planform are shown in Fig. 3. Negative velocity contours are evident toward the centerline of the planform, clearly demonstrating the attachment of the leading-edge separated flow. A direct comparison with crossflow streamlines at both x/c locations corroborates this interpretation. The highest peaks in the negative w contours designated by a are located directly under the positive

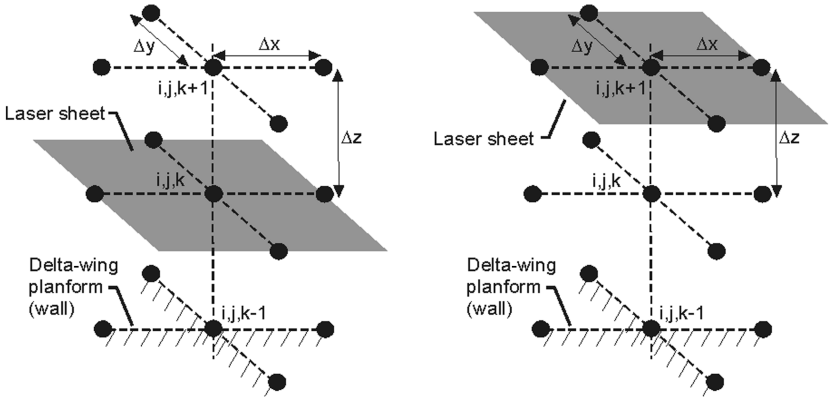

Fig. 2 Schematic of the nodes used in the discretization of the continuity equation, showing the location of the laser sheets at nodes a) (i, j, k) and b) $(i, j, k+1)$.

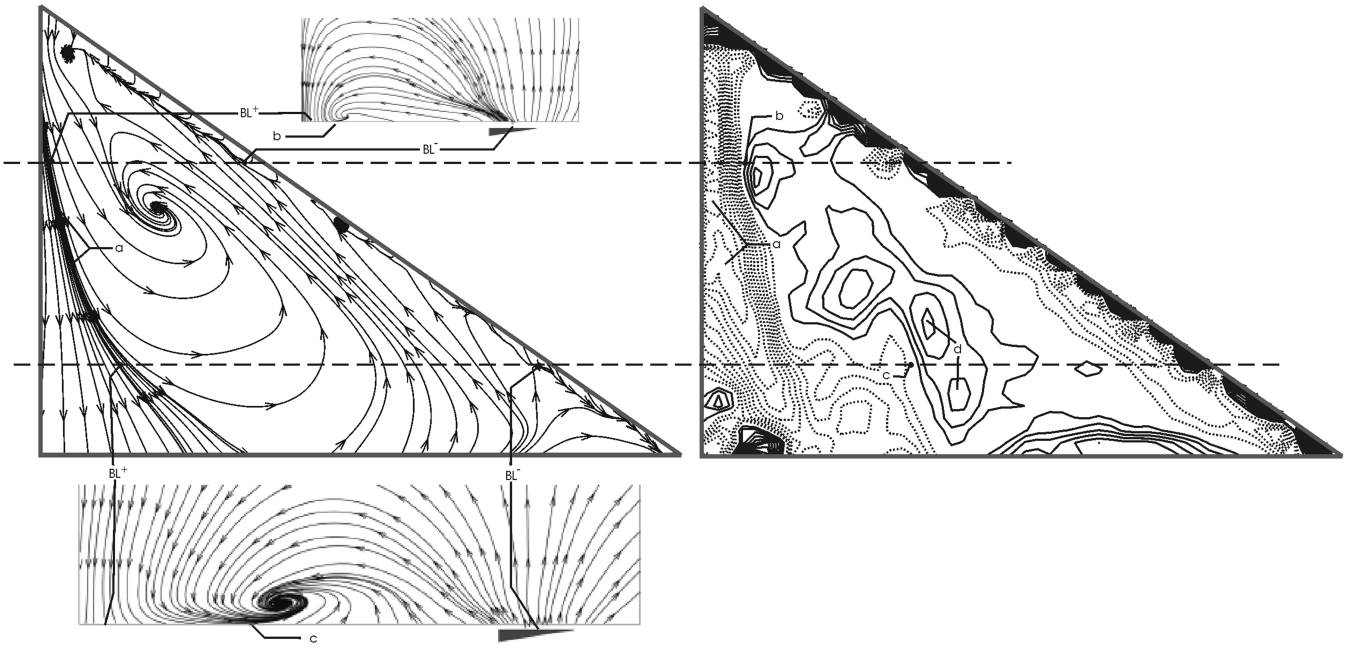

Fig. 3 Comparison of normal-to-plane motion w contours, near-surface streamlines, and crossflow patterns at $x/c = 0.34$ and 0.8 at a Reynolds number of $Re = 10,000$. Minimum and incremental values of w are -3.25 and 0.25 mm/s, respectively.

experimental bifurcation line BL^+. At $x/c = 0.34$, a zero velocity contour designated by b is apparent in both the present and the experimental results. Moving along the same x/c toward the leading edge of the planform, a region of decreasing positive w contours exists and is clearly verified by examining the corresponding crossflow streamline patterns. Further toward the leading edge, patches of negative w contours are detected at some locations, whereas positive concentrations of w contours are evident along the entire length of the leading edge of the planform. These concentrations correspond to the experimental crossflow streamlines emanating from the leading edge. At $x/c = 0.8$, the negative w contours spread over a wider area where the positive bifurcation line BL^+ starts smearing. The zero w velocity contour, labeled by c, moves outboard from the centerline of the planform and is manifested in the crossflow underneath the vortex core. To the right of this core, two positive peaks of w contours, designated by d, exist, resembling the roll up of the flow as depicted in the crossflow image. Moving further along the same x/c toward the leading edge, negative w contours are noticed inboard of the bifurcation line BL^-. However, no crossflow streamline correspondence is detected, which in turn might be attributed to the differences between the experimental setup of the crossflow imaging and the computed normal-to-plane velocity that is based on a different setup, as discussed at the beginning of this section. Furthermore, due to the reflection of the laser sheet in crossflow imaging, near-surface flow patterns in close vicinity to the planform are not resolved in which these negative w contours might have fallen. This is indicated by the blank region between the edge of the field of view and the surface, which typically varies between 0.6 and 1.5 mm. At the leading edge, starting around $x/c = 0.6$ and moving toward the tip of the planform, a clear correspondence between the negative bifurcation line BL^- and the positive w contours is evident, as they both follow a wavy trend at the same spatial location.

IV. Surface Shear Stress Lines of a Delta-Wing Planform

Similar to the normal-to-plane motion, the surface streamlines/shear stress lines are computed using the two laser sheet planes adjacent to the planform located at $z/c \approx 0.0051$ and $z/c \approx 0.0102$ away from the surface. The computed surface shear stress lines are compared with the experimental near-surface streamlines located at the aforementioned locations. It is worth noting that the data for the 1-mm plane is taken from Yavuz and Rockwell [6], whereas that of the $z/c \approx 0.0051$ plane has not been published and is provided to the authors through personal communication.

Surface shear stress lines along with near-surface streamlines at $z/c \approx 0.0051$ and $z/c \approx 0.0102$ are depicted in Figs. 4a–4c, respectively. A saddle point, designated as S_1 is observed in both the surface shear stress lines and the streamlines located 0.5 mm away from the surface at almost the same location, whereas no such pattern is observed at the corresponding location for the streamlines acquired

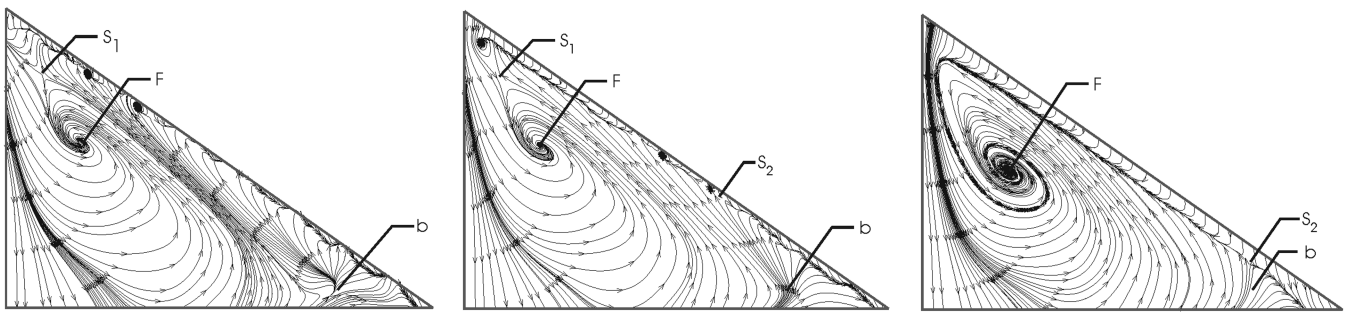

a) b) c)

Fig. 4 Comparison of a) surface shear stress lines, b) near-surface streamlines located at $z/c \approx 0.0051$, and c) $z/c \approx 0.0102$ from the planform at an angle-of-attack $\alpha = 10$ deg and a Reynolds number of $Re = 10,000$.

at the $z/c \approx 0.0102$ plane. Attachment lines follow closely the positive bifurcation lines of both the $z/c \approx 0.0051$ and the $z/c \approx 0.0102$ planes. A focus designated as F is clearly evident at the surface and at both near-surface planes and moves toward the trailing edge with an increase in elevation. An attachment line designated by b is apparent at the surface where multiple shear stress lines emanate toward the leading edge. This attachment line disperses in the $z/c \approx 0.0051$ plane and almost diminishes in the $z/c \approx 0.0102$ plane. The separation line in Fig. 4a, running along the leading edge of the planform, has a prevailing direction away from the apex and toward the tip of the planform. At the $z/c \approx 0.0051$ plane, a saddle point designated as S_2 appears in the negative bifurcation line at an $x/c \approx 0.78$, splitting the direction of the streamlines. This saddle point in the $z/c \approx 0.0102$ plane moves further toward the tip of the planform and is observed at an $x/c \approx 0.84$. The separation shear stress line is extremely close to the leading edge of the planform, which corresponds to the separating shear layer emanating from the leading edge of the planform. The negative bifurcation line, which corresponds to this shear stress line, at both planes adjacent to the surface, moves inboard and to a greater extent at the $z/c \approx 0.0102$ plane.

V. Conclusions

The normal-to-plane motion adjacent to a delta-wing planform, at the $z/c \approx 0.0051$ plane, has been computed using a simple finite difference scheme and assessed against streamlines acquired at the same location for a delta wing having a low sweep angle ($\Lambda = 35$ deg). The computed w contours were also compared with experimental crossflow patterns at two different x/c locations. Using the same technique, surface shear stress lines were computed and assessed against near-surface streamlines at both $z/c \approx 0.0051$ and $z/c \approx 0.00102$ away from the surface. The principal findings are as follows:

1) Surface shear stress lines differ from patterns of time-averaged streamlines adjacent to the planform located at $z/c \approx 0.0051$ and $z/c \approx 0.00102$ from the surface, demonstrating the effect of the pressure gradient accompanied by an error of a second order as a result of the discretization process. The separation line moves inboard away from the leading edge with increasing elevation and is accompanied by an outboard motion of the associated saddle point toward the tip of the planform.

2) Normal-to-plane patterns of w contours computed at the $z/c \approx 0.0051$ plane show remarkable similarities to near-surface streamlines at the same location and to patterns of crossflow streamlines when qualitatively assessed at two streamwise locations.

Acknowledgments

The authors would like to thank Donald Rockwell and Metin Yavuz for providing the experimental data.

References

[1] Gordnier, R. E., and Visbal, M. R., "Higher-Order Compact Difference Scheme Applied to the Simulation of a Low Sweep Delta Wing Flow," AIAA Paper 2003-0620, Jan. 2003.

[2] Taylor, G. S., and Gursul, I., "Unsteady Vortex Flows and Buffeting of a Low Sweep Delta Wing," AIAA Paper 2004-1066, Jan. 2004.

[3] Ol, M. V., and Gharib, M., "The Passage Towards Stall of Nonslender Delta Wings at Low Reynolds Number," AIAA Paper 2001-2843, June 2001.

[4] Yavuz, M. M., Elkhoury, M., and Rockwell, D., "Near-Surface Topology and Flow Structure on a Delta Wing," *AIAA Journal*, Vol. 42, No. 2, 2004, pp. 332–340. doi:10.2514/1.3499

[5] Yavuz, M. M., and Rockwell, D., "Control of Flow Structure on Delta Wing with Steady Trailing-Edge Blowing," *AIAA Journal*, Vol. 44, No. 3, 2006, pp. 493–501. doi:10.2514/1.16444

[6] Yavuz, M. M., and Rockwell, D., "Identification and Control of Three-Dimensional Separation on Low Swept Delta Wing," *AIAA Journal*, Vol. 44, No. 11, 2006, pp. 2805–2811. doi:10.2514/1.24756

[7] Elkhoury, M., Yavuz, M. M., and Rockwell, D., "Near-Surface Topology of Unmanned Combat Air Vehicle Planform: Reynolds Number Dependence," *Journal of Aircraft*, Vol. 42, No. 5, 2005, pp. 1318–1330. doi:10.2514/1.9777

[8] Squire, L. C., "The Motion of a Thin Oil Sheet Under the Boundary Layer on a Body," AGARDOgraph 70, 1962.